Immunologic Research (2024) 72:797–810
https://doi.org/10.1007/s12026-024-09486-5

RESEARCH

Inhibition of LSD1 via SP2509 attenuated the progression of rheumatoid arthritis

Ziliang Yu[1] · Peipei Li[2] · Dagong Gao[1] · Yalong Hu[3] · Fei Xia[1] · Lei Liu[1] · Jian Liu[1] · Wei Liu[1] · Haiping Zhang[1]

Received: 28 March 2024 / Accepted: 29 April 2024 / Published online: 9 May 2024

Abstract

Rheumatoid arthritis (RA) is a chronic autoimmune disease characterized by synovial hyperplasia, pannus formation, and cartilage and bone destruction. Lysine-specific demethylase 1 (LSD1), an enzyme involved in transcriptional regulation, has an unclear role in synovial inflammation, fibroblast-like synoviocytes migration, and invasion during RA pathogenesis. In this study, we observed increased LSD1 expression in RA synovial tissues and in TNF-α-stimulated MH7A cells. SP2509, an LSD1 antagonist, directly reduced LSD1 expression and reversed the elevated levels of proteins associated with inflammation, apoptosis, proliferation, and autophagy induced by TNF-α. Furthermore, SP2509 inhibited the migratory capacity of MH7A cells, which was enhanced by TNF-α. In CIA models, SP2509 treatment ameliorated RA development, reducing the expression of pro-inflammatory cytokines and alleviating joint pathological symptoms. These findings underscore the significance of LSD1 in RA and propose the therapeutic potential of SP2509.

Keywords Rheumatoid arthritis · LSD1 · SP2509 · MH7A

Introduction

Rheumatoid arthritis (RA) represents a chronic and intricate autoimmune disease, distinguished by synovial hyperplasia, pannus formation, and the relentless destruction of bone and cartilage. Afflicting a considerable portion of the global population, RA patients endure a persistent and fluctuating disease course, ultimately leading to joint malfunction and deformity, significantly compromising their quality of life [1, 2]. Astonishingly, an estimated 17,600,000 people in 2020 had rheumatoid arthritis worldwide according to RA prevalence research [3]. Inadequate management of rheumatoid arthritis may exacerbate its progression, culminating in irreversible disability and imposing substantial socio-economic burdens [4].

Nonetheless, the intricate cellular and molecular mechanisms underlying RA pathogenesis remain enigmatic. Among various cell types driving RA progression, fibroblast-like synoviocytes (SFs), T lymphocytes, B lymphocytes, monocytes, and neutrophils play crucial roles, with particular emphasis on SFs and macrophages [5–7]. These rheumatoid arthritis synovial fibroblasts (RASF), which, under healthy conditions, contribute to synovial homeostasis, are deemed central to joint destruction when they collaborate with other mesenchymal and immunocompetent cells [8, 9]. A mounting body of evidence underscores the pivotal role of SFs in RA, as they produce an array of pro-inflammatory cytokines like interleukin IL-6, IL-1β, tumor necrosis factor (TNF)-α, inducible nitric oxide synthase (INOS), and proteinases, notably matrix metalloproteinases (MMPs) [10, 11]. These inflammatory mediators perpetuate joint destruction, propelling the quest for research aimed at inhibiting RASFs activation as a potential therapeutic strategy for treating rheumatoid arthritis.

Lysine-specific demethylase 1 (LSD1), also known as KDM1, stands as the pioneering histone demethylase

✉ Wei Liu
liuweidr@yeah.net

✉ Haiping Zhang
zhanghaipingx@163.com

1 Department of Orthopaedics, Nantong First People's Hospital, Affiliated Hospital 2 of Nantong University, No.666 Shengli Road, Nantong 226000, Jiangsu, China

2 Department of Operating Room, Nantong First People's Hospital, Affiliated Hospital 2 of Nantong University, Nantong 226000, Jiangsu, China

3 Department of Orthopaedics, Qidong People's Hospital, Affiliated Qidong Hospital of Nantong University, Nantong 226000, Jiangsu, China

identified within the superfamily of flavin adenine dinucleotide (FAD)-dependent amine oxidases [12]. Through its FAD-dependent amine oxidase activity, LSD1 specifically demethylates mono- and di-methylated H3K4, thereby repressing gene expression by eliminating active histone marks (H3K4me2) from gene promoter regions [13]. This multifaceted enzyme plays a pivotal role in diverse physiological processes, encompassing hematopoiesis, adipogenesis, developmental processes, DNA methylation maintenance, and, prominently, cancer development, where it fosters cancer cell survival and fosters a cancer-friendly microenvironment [14–16]. Consequently, targeting LSD1 for inhibition emerges as an alluring strategy to curb cancer progression. In addition, LSD1 extends its involvement beyond cancer, contributing to the development of diverse pathological conditions or diseases. One such instance involves its regulation of the inflammatory response by governing the expression of various cytokine genes. In acute and severe inflammatory conditions, inhibiting LSD1 activity curtails inflammation spread, as evidenced by findings from a cecal ligation and puncture (CLP)-mediated sepsis mouse model [17]. Downregulation of LSD1 in CD4 + T cells resulted in reduced secretion of IFN-γ and IL-17, while increasing IL-10 levels, which led to impaired proliferation of CD4 + T cells, ultimately alleviating the severity of rheumatoid arthritis [18]. However, the impact of LSD1 on RASFs has not been clearly illustrated.

This study examined LSD1 expression in healthy, osteoarthritis (OA), and RA synovial tissues, confirming elevated levels in RA. Using SP2509 to inhibit LSD1, we successfully reversed the heightened levels of proteins associated with inflammation, apoptosis, proliferation, and autophagy triggered by TNF-α. Additionally, SP2509 mitigated the migratory capacity of MH7A cells, which had been increased by TNF-α. In collagen-induced arthritis (CIA) models, SP2509 treatment ameliorated RA development, lowering pro-inflammatory cytokine expression and improving joint pathology. These findings highlight LSD1's significance in RA and suggest SP2509 as a potential therapeutic option.

Materials and methods

Patients and tissue samples

Human synovial tissues were procured from six rheumatoid arthritis (RA) patients who underwent total knee or total hip arthroplasty at the Department of Orthopedics, Affiliated Hospital 2 of Nantong University. As controls, synovial tissues were also collected from six healthy individuals during arthroscopic surgery. The average age of RA patients was 48 ± 6.3 years, while that of the control group was 46 ± 5.6 years. The current study was conducted in strict adherence to the protocols and procedures reviewed and approved by the institutional medical ethics committee of the Second Affiliated Hospital of Nantong University. Prior to any treatment, informed consent was meticulously obtained in written format from each recruited subject.

GEO datasets analysis

GSE89408 datasets were downloaded from the GEO database, encompassing total RNA sequencing data from synovial biopsies of subjects with and without RA [19, 20]. RNA counts from 28 healthy tissues and 152 RA tissues were then meticulously separated and analyzed to investigate LSD1 expression differences. The RA samples were further categorized into high and low LSD1 expression groups based on the median expression of LSD1. Differentially expressed genes (DEGs) were identified between these groups using the DeSeq2 method, with the criteria of |log2FoldChange| > 1 and an adjusted p value < 0.01.

The DEGs were subsequently subjected to gene ontology (GO) enrichment analysis and Kyoto Encyclopedia of Genes and Genomes (KEGG) pathway analysis. For deeper insights into the pathways associated with LSD1 expression levels in RA, we performed gene set enrichment analysis (GSEA) using version 4.0.3 of the software (http://www.broadinstitute.org/gsea) with c2.cp.kegg.v7.1.symbols.gmt gene set from Human_ENSEMBL_Gene_ID_MSigDB.v7.0. Enrichment scores were calculated, and the GSEA program was executed with 1000 permutations to assess the statistical significance. A significance threshold of $p < 0.01$ was applied to identify pathways that were significantly linked to LSD1 expression in RA.

Cell culture and stimulation

MH7A cells were procured from Shanghai Guandao Biotechnology Co., Ltd., Shanghai, China, and were cultured in either high glucose Dulbecco's modified Eagle's medium (DMEM; Thermo Fisher Scientific, USA) or minimal essential medium (MEM; Thermo Fisher Scientific). The culture medium consisted of 10% fetal bovine serum (FBS; Gbico, USA), 100 U/ml penicillin, and 100 μg/ml streptomycin, and the cells were maintained in an atmosphere containing 5% CO_2 at 37 °C. Regular medium change was carried out every 2 days, and cell passaging was performed once the degree of cell confluence reached above 90%. For the present investigation, cells at passages 3–8 were utilized. TNF-α (Sigma, USA) and SP2509 (AdooQ, A14443, China) were employed for stimulating the cells at the corresponding concentration for 24 h before further assay. The structure of SP2509 is illustrated in Figure S1.

Immunohistochemical analysis

Fresh synovial tissues were meticulously fixed with 4% paraformaldehyde at 4 °C overnight, followed by embedding in paraffin and subsequent sectioning into 5-μm slices. These sections underwent a series of meticulous procedures, including immersion in xylene thrice for 10 min each, dehydration using different concentrations of ethanol, and thorough rinsing with water. Antigen restoration was achieved using sodium citrate, and endogenous peroxidase activity was effectively blocked for 30 min. Subsequently, the sections were incubated overnight at 4 °C with anti-LSD1 antibody (1:100, 20183-1-AP, ProteinTech, China), followed by a 30-min incubation at room temperature with the respective horseradish peroxidase (HRP)-conjugated secondary antibodies (1:400, Abcam, USA). The sections were then subjected to 3,3′-diaminobenzidine (DAB) staining, followed by hydrochloric acid color-separation for 3–5 min. After a counterstain with hematoxylin for 20–30 s, a 10-min rinse with running water was performed, followed by a repetition of the dehydration step. Finally, the sections were air-dried and sealed, and the stained sections were meticulously examined using a microscope (Zeiss axio imager m2, Germany).

Western blot analysis

Total protein extraction was conducted using radioimmunoprecipitation assay (RIPA) lysis buffer (Beyotime, Shanghai, China), supplemented with protease inhibitors and a phosphatase inhibitor cocktail (Boster Biotechnology). Subsequently, equal amounts of protein were meticulously separated by 10% sodium dodecyl sulfate polyacrylamide gel electrophoresis (SDS-PAGE) and transferred to a polyvinylidene fluoride (PVDF) membrane. The PVDF membrane was blocked with 5% skim milk in a Tris-buffered saline with 0.1% Tween 20 buffer (TBST), and the corresponding primary antibodies were incubated overnight at 4 °C. After meticulous washing with TBST, the membrane was subjected to a 120-min incubation with appropriate horseradish peroxidase-conjugated secondary antibodies. The specific information of antibodies was shown in Supplementary Table 1. Ultimately, an enhanced chemiluminescence detection system (Thermo Fisher Scientific, Waltham, MA, USA) in combination with the ChemiDoc Touch Imaging System (BioRad Laboratories, Hercules, CA, USA) was employed for the identification of antibody-bound proteins. The quantification of protein levels was accomplished using ImageJ software and subsequently normalized to the control.

The knockdown of LSD1 with siRNA transfection

The LSD1 expression in FLSs was knocked down with human LSD1 siRNA (siLSD1), and the processed siRNA was applied as a negative control (siNC) (RiboBio, Shanghai, China). The transient transfection of siRNA was meticulously carried out employing riboFECTTM CP Reagent (RiboBio, Shanghai, China), strictly following the manufacturer's instructions. Subsequent to siRNA transfection, the cells were subjected to a 6-h incubation and cultured in serum-free medium, followed by transfer to total medium containing 10% FBS for an additional 48 h. Upon validation of successful LSD1 knockdown, the cells were prepared for further experimental procedures.

Cell scratch and transwell assay

MH7A cell migration was assessed using the scratch-wound healing method. In brief, MH7A cells were seeded in 6-well plates with ample nutrition. When the cells reached approximately 90% confluence, they were transferred into serum-free medium. Subsequently, linear scratch wounds were meticulously created using 200-μl pipette tips, and MH7A cells were then subjected to different treatments: SP2509 and TNF-α, or TNF-α alone without SP2509. The scratched areas were captured at 0 and 24 h using a microscope (Nikon, Tokyo, Japan), and the migratory ability of the cells, represented by the wound healing percentage, was meticulously calculated utilizing ImageJ software. The wound healing percentage was computed as follows: [(0 h wound width − 24 h wound width)/0 h wound width] × 100%.

For the Transwell assay, MH7A cells were suspended in 200 μl serum-free medium at a concentration of 6×10^4 cells/ml and plated in the upper wells of Boyden chambers (8.0 μm pore, Corning, USA) without Matrigel (BD Bioscience, USA). The bottom wells were supplemented with 600 μl DMEM medium containing 10% FBS. Following 24 h of incubation, the upper chamber was fixed with methanol and stained with 0.1% crystal violet. Subsequently, photographs were taken, and the cells that migrated or invaded the back of the chamber were meticulously counted. For accurate results, five random fields were selected to calculate the number of migrating cells.

Animal experiments

Female DBA/1 mice, aged 6 weeks, were selected as the experimental subjects for this study. These mice were housed under constant environmental conditions, maintaining a temperature of 23 ± 1 °C, with a 12-h light-dark cycle. They were provided with unrestricted access to water and food throughout the study. To induce arthritis, bovine type II collagen (2 mg/ml in 0.05 M acetic acid; Chondrex, Inc., Redmond, WA, USA) was mixed with an equal volume of Freund complete adjuvant (2 mg/ml Mycobacterium tuberculosis; Chondrex, Inc.). On the

first day of the experiment, 100 µg of bovine type II collagen was intradermally injected at the base of the mice's tails. On day 21, a booster intradermal injection of 100 µg of bovine type II collagen, emulsified with an equal volume of incomplete Freund adjuvant (Chondrex, Inc.), was administered. Subsequently, the mice were randomly divided into four groups: control, CIA, SP2509 low-dose, and SP2509 high-dose groups. To assess the impact of SP2509 on arthritis development, the mice received intraperitoneal administration of SP2509 at doses of 25 or 50 mg/kg body weight (low and high doses, respectively) four times per week for 4 weeks after the booster injection.

The incidence, severity, and progression of arthritis were meticulously assessed every 2 days following booster immunization by meticulously determining the arthritis score and meticulously measuring the posterior paw thickness and body weight of the mice. The paws were allocated clinical scores as per the following criteria [21]: 0 for normal condition, 1 for mild swelling of the ankle or wrist without deformities and erythema, 2 for moderate redness and swelling of the ankle or wrist, 3 for severe redness and swelling of the entire paw, including the digits, and 4 for severe erythema and swelling of the limb or ankylosis. The degree of paw swelling was meticulously evaluated by precisely measuring the paw thickness using vernier calipers.

After 49 days, the animals were anesthetized and humanely euthanized for further analysis. The knee joints of the mice were meticulously fixed in paraformaldehyde and subjected to a decalcification process lasting 4 weeks. For comprehensive histological evaluation, the samples were meticulously embedded in paraffin and subsequently sectioned at a thickness of 5 µm. The tissue sections were stained with hematoxylin and eosin (HE), enabling a systematic scoring of synovial inflammation, as well as cartilage and bone destruction, following a grading system as follows: 0 for no significant change, 1 for mild change, 2 for moderate change, and 3 for severe change. Moreover, the extent of articular cartilage damage was thoroughly assessed utilizing the modified International Osteoarthritis Research Association (OARSI) scoring system.

The study has received approval from the Laboratory Animal Center of Nantong University.

Enzyme-Linked Immunosorbent Assay (ELISA)

In order to investigate the impact of SP2509 on the in vivo secretion of pro-inflammatory cytokines, serum samples were collected on day 49 and subsequently stored at −80 °C until analysis. The levels of TNF-α, IL-6, and IL-1β in the serum were quantified following the guidelines provided by the manufacturer.

Statistical analysis

The data are expressed as means ± standard deviation (SD). Statistical analysis was conducted using Prism software (version 9.0; GraphPad Software). All experimental data were independently repeated at least three times to ensure reliability and accuracy. The statistical evaluation involved one-way analysis of variance (ANOVA) followed by the Tukey test for multiple comparisons. A p value less than 0.05 was considered to indicate statistical significance.

Results

Upregulated expression and activation of LSD1 in synovial tissues of rheumatoid arthritis patients

Based on the analysis of the GSE89408 datasets, it was observed that RNA counts of LSD1 were notably elevated in rheumatoid arthritis (RA) tissues compared to healthy tissues (Fig. 1A). To investigate the associations among LSD1 expression, downstream genes, and related pathways, RA samples were stratified into high and low expression groups based on their LSD1 levels. Subsequently, differentially expressed genes (DEGs) in these two groups were identified and visualized in the volcano plot (Fig. 1B). The expression patterns of the top 11 upregulated and the top 11 downregulated genes are listed in Supplementary Tables 2 and illustrated in Fig. 1C. Notably, the upregulated genes, such as matrix metalloproteinase 1 (MMP1), matrix metalloproteinase 3 (MMP3), and interleukin-8 (IL-8), are well-known contributors to RA progression [22]. Furthermore, DEGs underwent enrichment analysis using GO, KEGG, and GSEA methods. These analyses revealed the downregulations of pathways related to functions, like haptoglobin binding, actin binding, calcium signaling pathway, hemostasis, and innate immune system (Fig. 2, Supplementary Tables 3 and 4), all have been previously associated with RA progression [23–29], indirectly supporting the involvement of LSD1.

To reinforce these findings, we conducted an additional analysis using synovial tissues obtained from RA and osteoarthritis (OA) patients using western blot and immunohistochemistry assays. It confirmed a significant increase in LSD1 protein levels, as well as MMP9 and INOS, in RA synovial tissues compared to those of OA patients (Fig. 3A and B). This observation was further supported by immunohistochemistry assays, which demonstrated an overexpression of LSD1 in synovial sections from RA patients in comparison to those from OA patients, as evident in Fig. 3C and D.

Moreover, upon establishment of the in vitro model, stimulating MH7A cells with TNF-α, we observed a time-dependent increase in the expression of specific proteins

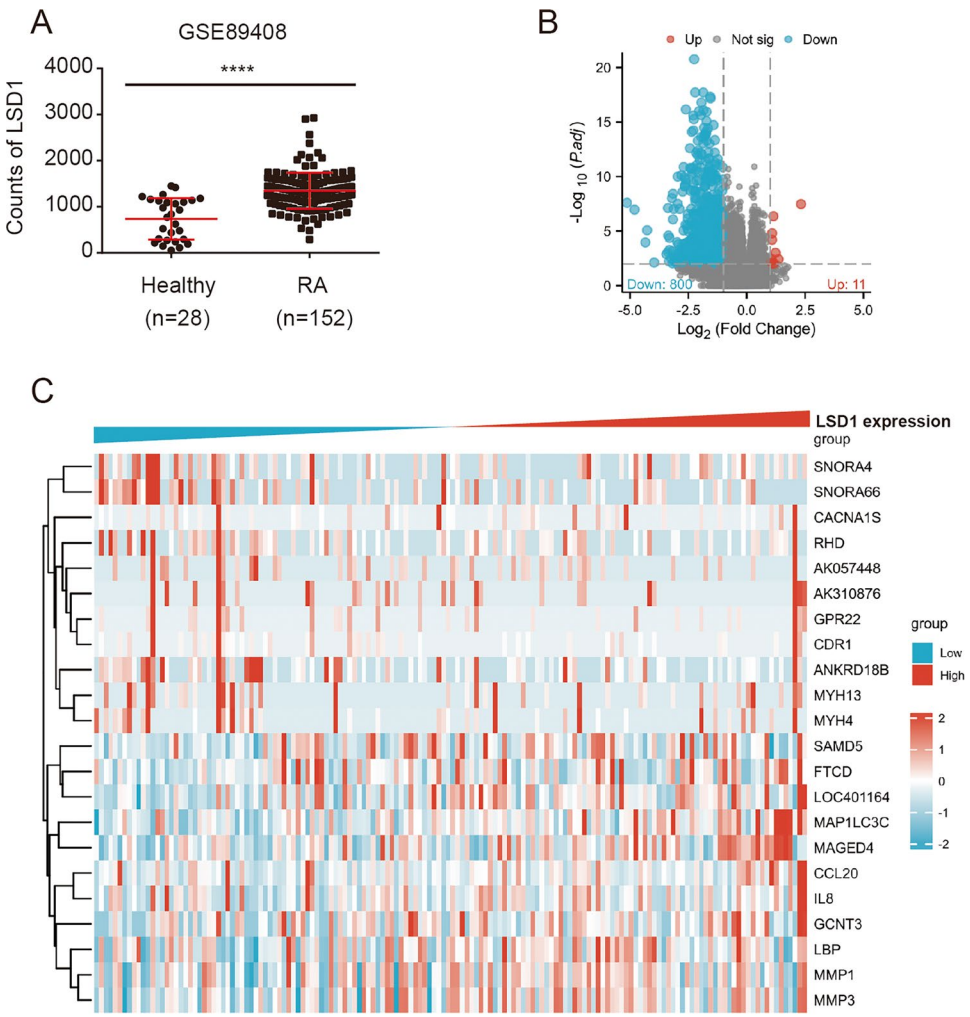

Fig. 1 Screening of differentially expressed genes in RA tissues associated with LSD1 expression. **A** RNA counts of LSD1 in healthy and RA tissues are analyzed. **B** Volcano plots show the differentially expressed genes in RA tissues with high LSD1 expression compared to low LSD1 expression. **C** Top 22 dysregulated genes are presented in heatmap. Data is presented as mean ± SD. ****$p < 0.0001$

(Fig. 4). These proteins, including MMP2, MMP9, INOS, LSD1, and IL-1β, showed a notable upregulation in response to TNF-α stimulation, which rose progressively within a 12-h time period.

SP2509 affects inflammatory response, apoptosis, and autophagy in MH7A cells by downregulating LSD 1

To further investigate the impact of LSD1 on RA cells, we utilized the antagonist of LSD1, SP2509, to modulate the expression of LSD1 in MH7A cells. A dose-dependent downregulation of LSD1 was observed after treatment of SP2509, as well as INOS and Cyclooxygenase-2 (COX-2), which were upregulated via TNF-α treatment compared to the blank control treated with the DMSO (Fig. 5A and B), supporting that SP2509 effectively downregulated LSD1 expression in MH7A cells and inhibited the inflammatory response induced by TNF-α. Intriguingly, after employing LSD1 small interfering RNA to transfect MH7A cells, the downregulation of LSD1 coincided with a corresponding decrease in INOS expression was observed, further substantiating the inhibitory effect of LSD1 inhibition on inflammatory factors (Figure S2).

Moreover, the expression of proteins associated with cell proliferation and apoptosis, including Bcl-2, BCL2 associated X (Bax), proliferating cell nuclear antigen (PCNA) and Caspase3, was also detected after treatment of MH7A with TNF-α and SP2509 (Fig. 5C and D). As the concentration of SP2509 increased, there was a noticeable rise in the expression of Bax protein, a pivotal regulator of apoptosis, while the expression of Bcl2 protein, known for its anti-apoptotic properties, exhibited a decline. Remarkably, the expression of caspase3 increased in tandem with the concentration of SP2509, also providing additional evidence for the potential role of SP2509 in inducing apoptosis in MH7A cells. Moreover, as the concentration of SP2509 escalated, a concomitant decrease in proliferating cell nuclear antigen (PCNA) expression was observed, further supporting the notion that SP2509 may suppress cell proliferation.

To unravel the intricate interplay between SP2509 and autophagy, which plays a crucial role in cellular responses,

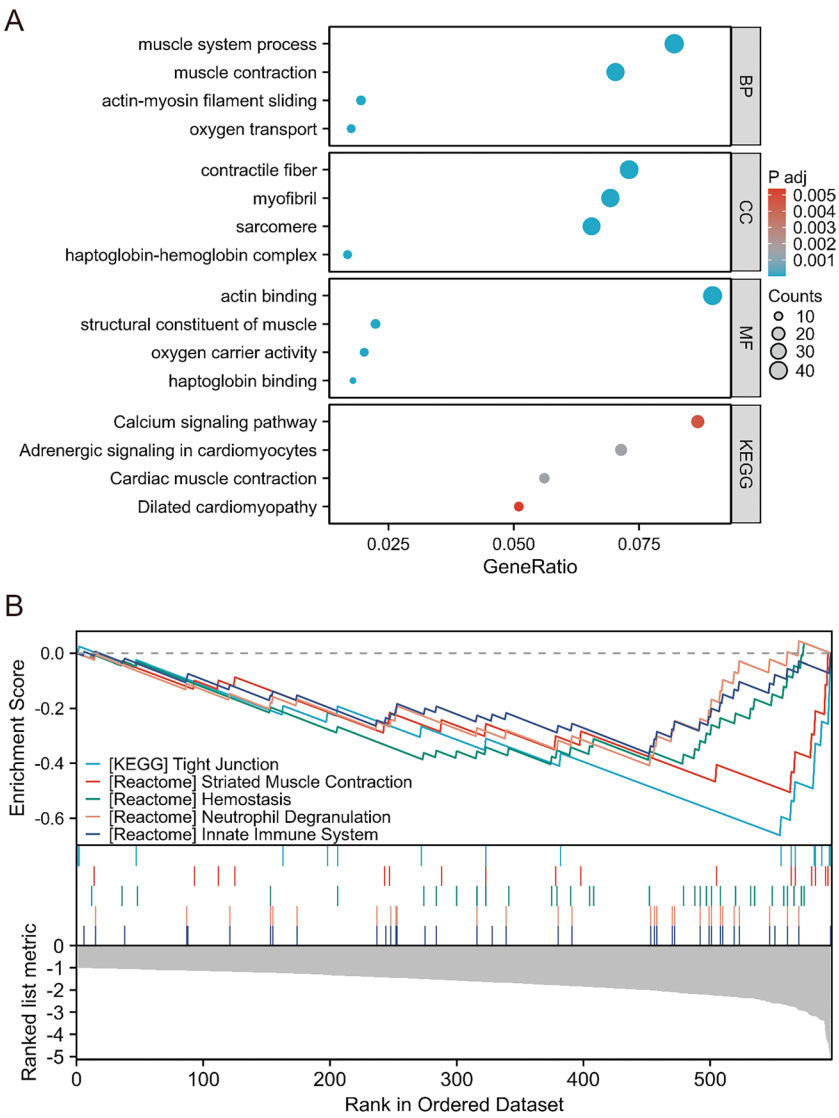

Fig. 2 The aberrantly expressed pathways associated with LSD1 expression. **A** GO and KEGG analysis is performed for enriching downregulated genes in RA tissues with high LSD1 expression. **B** GSEA enrichment is performed to screen the relevant pathways

we assessed the expression of key autophagy-related marker proteins, including LC3I/II, Beclin1, autophagy related 5 (ATG5), and autophagy related 7 (ATG7), within the TNF-α-induced MH7A cell model (Fig. 5E and F). Astonishingly, as the concentration of SP2509 increased, a discernible decrease in the expression of these autophagy-related proteins was observed. This intriguing observation implies that SP2509 may impede the autophagy process in MH7A cells.

SP2509 reduced the migrative abilities of TNF-treated MH7As

Matrix metalloproteinases (MMPs) constitute a family of zinc-dependent proteases that hold clinical relevance, particularly due to elevated levels observed in patients with RA. In RA, cartilage destruction is a defining characteristic, with the secretion of MMPs by RAFLs playing a pivotal role. As shown in Fig. 6, the protein levels of MMP2 and MMP9 evaluated by stimulation of TNF-α displayed a notable reduction in a concentration-dependent manner upon treatment with SP2509. Thus, inhibition of LSD1 may be a potential strategy for suppressing MMP2 and MMP9 and preventing the destruction of RA cartilage.

To accurately evaluate MH7A cell migration, we conducted wound healing and Transwell assays with or without the presence of SP2509. The introduction of TNF-α notably accelerated the wound healing rate of MH7A cells, which was effectively reversed by SP2509 treatment (Fig. 7A and C). Importantly, as the concentration of SP2509 increased, the wound healing rate exhibited a dose-dependent decrease. In line with these findings, the quantity of cells that migrated and adhered to the membrane in the lower Transwell chamber, which had increased due to TNF-α treatment, was also dose-dependently reduced by SP2509 (Fig. 7B and D). However, due to the apoptosis-promoting effects of SP2509 on RASFs, the

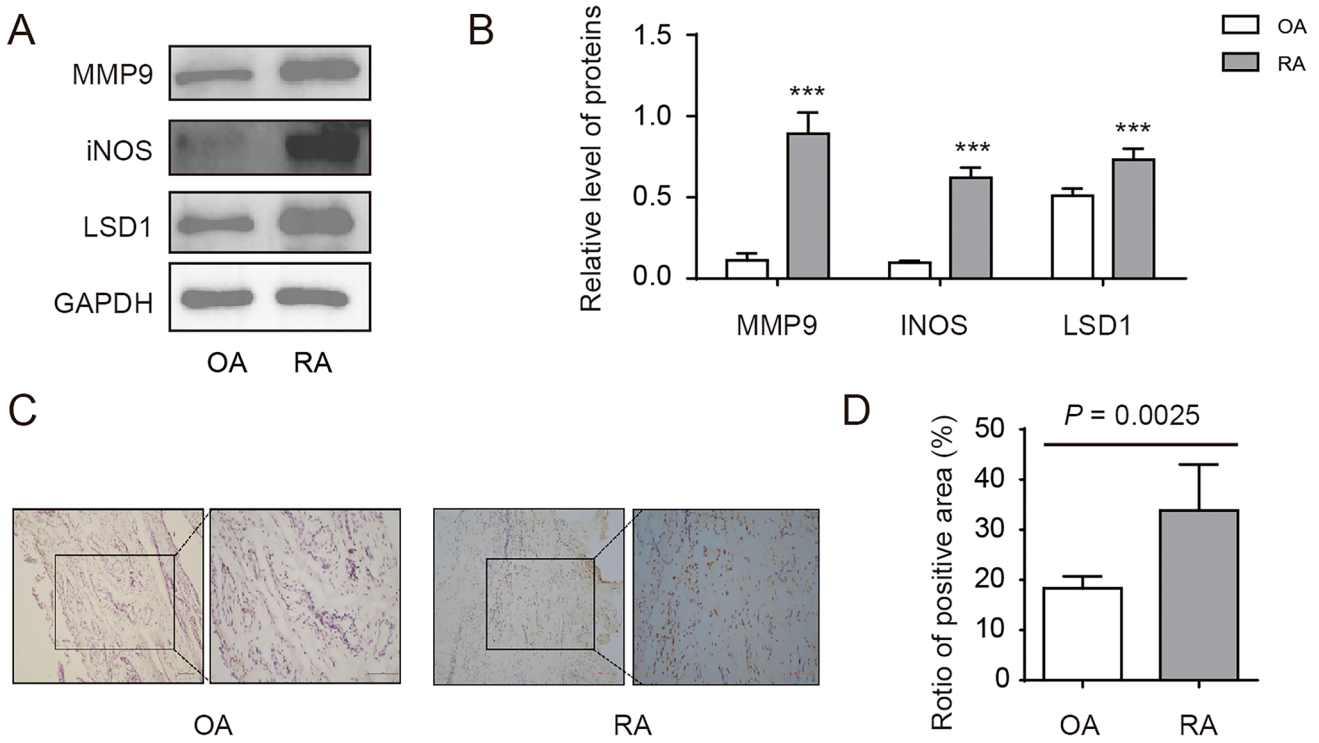

Fig. 3 Protein level of LSD1 is upregulated in RA tissues compared to OA tissues. **A** Western blot detection of the expression of LSD1 and related inflammatory molecules in the articular process tissues of patients in the OA group and the RA group. **B** The histogram shows the relative expression ratio of LSD1, MMP9, and INOS. **C** Immunohistochemical detection of the expression of LSD1 in the synovial tissues of OA patients and knee joints of RA patients (scale bar = 100 μm). **D** Histogram showing quantification of LSD1 staining. Data is presented as mean ± SD. ***$p < 0.001$

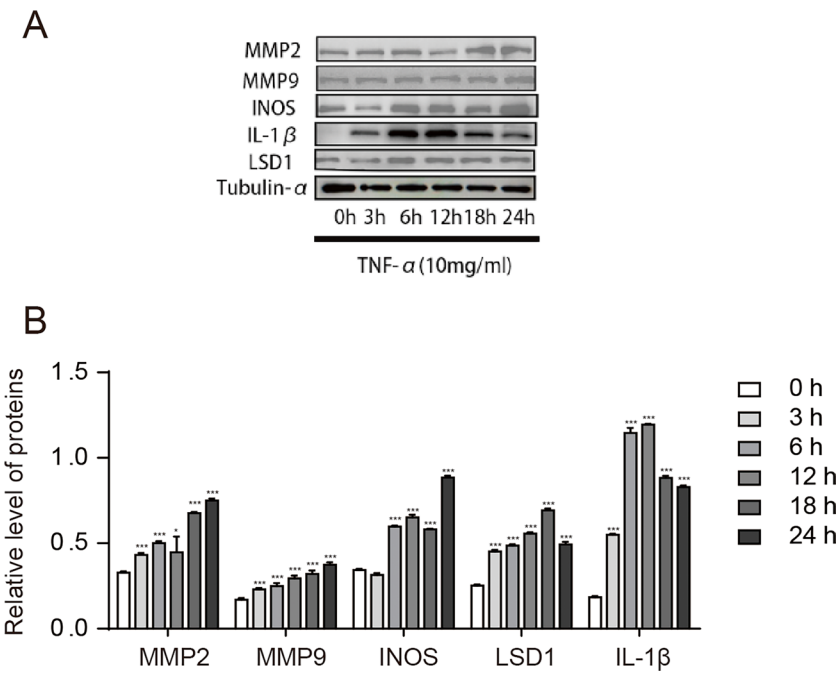

Fig. 4 Stimulation of TNF-α elevated expression of INOS, IL-1β, MMP2, MMP9, and LSD1 in MH7A cells. **A** After treatment with TNF-α for corresponding time, the expressions of INOS, IL-1β, MMP2, MMP9, and LSD1 in MH7A cells are detected by western blot method. **B** The histogram shows the relative expression ratio of INOS, IL-1β, MMP2, MMP9 and LSD1. Data is presented as mean ± SD for three independent assays. ***$p < 0.001$

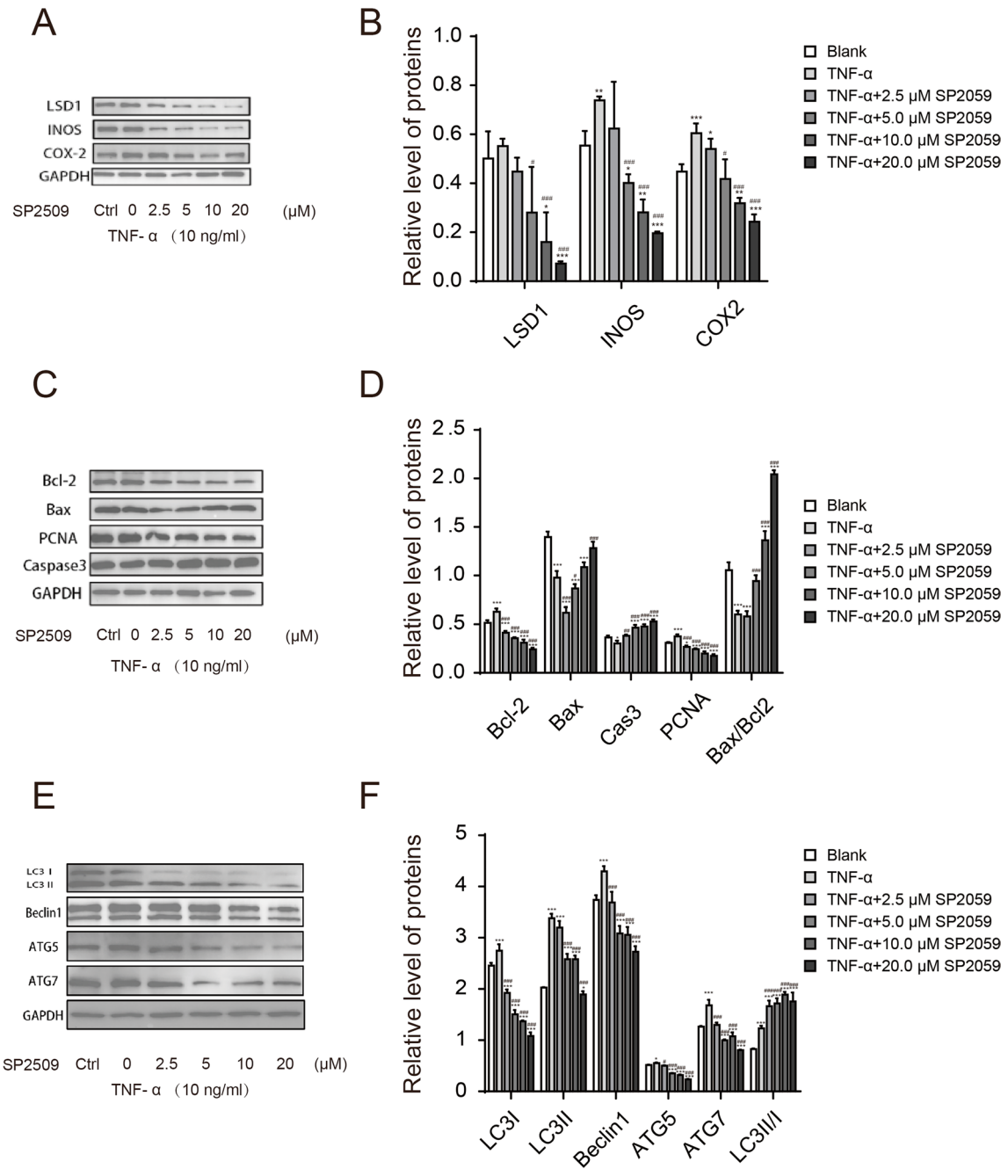

Fig. 5 SP2509 reversed the effects on cell proliferation, apoptosis, inflammation, and autophagy induced by TNF-α in MH7A. **A** Detection of LSD1, INOS, and COX-2 expressions is performed with western blot method in MH7A cells treated by TNF-α and SP2509. **B** The histogram shows the relative expression ratio of LSD1, INOS, and COX-2. **C** Expression of apoptosis-associated proteins including Bcl-2, Bax, PCNA, and Caspase3 is detected with western blot method in MH7A cells treated by TNF-α and SP2509. **D** The histogram shows the relative expression ratio of Bcl-2, Bax, PCNA, and Caspase3. **E** The expression of apoptosis-associated proteins including LC3, Beclin1, ATG5, and ATG7 is detected with western blot method in MH7A cells treated by TNF-α and SP2509. **F** The histogram shows the relative expression ratio of LC3, Beclin1, ATG5, and ATG7. Data is presented as mean ± SD for three independent assays. $*p<0.05$, $**p<0.01$, $***p<0.001$ compared to the Blank group. $\#p<0.05$, $\#\#p<0.01$, $\#\#\#p<0.001$ compared to the TNF-α group

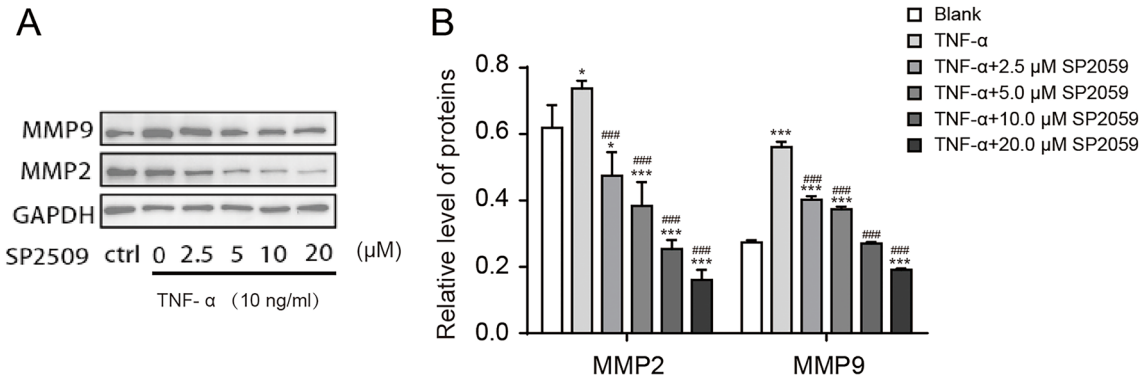

Fig. 6 SP2509 decreased the protein level of MMP2 and MMP9 in MH7A. **A** The detection of MMP2 and MMP9 expressions is performed with western blot method in MH7A cells treated by TNF-α and SP2509. **B** The histogram shows the relative expression ratio of MMP2 and MMP9. Data is presented as mean ± SD for three independent assays. *$p < 0.05$, **$p < 0.01$, ***$p < 0.001$ compared to the Blank group. #$p < 0.05$, ##$p < 0.01$, ###$p < 0.001$ compared to the TNF-α group

results of Transwell assay are influenced by the reduced cell number in upper chamber.

SP2509 ameliorates disease progression in mice with CIA

To ascertain the potential inhibitory effect of SP2509 on arthritis in vivo, we employed a CIA model in DBA-1 mice to evaluate its anti-arthritic properties. The experimental setup involved intradermal injections of 100 μg of bovine type II collagen on day 1, followed by a booster injection on day 21 using 100 μg of bovine type II collagen emulsified with an equal amount of incomplete Freund's adjuvant (Chondrex, Inc.). Subsequently, to assess the impact of SP2509 on arthritis development, the mice were intraperitoneally injected with either 25 or 50 mg/kg of SP2509 (designated as low and high doses, respectively) on a weekly basis for 4 weeks following the booster injection. The process was illustrated in Fig. 8A. Throughout the experimental period, the paws of the mice were photographed every 2 days, and their body weight and paw thickness were recorded. On the 48th day, the animals were anesthetized and euthanized, and both mouse serum and knee joint tissues were collected for subsequent ELISA and HE staining experiments.

Representative paw images from each group are displayed in Fig. 8B, highlighting the lesser degree of paw swelling in the SP2509 low-dose and high-dose groups compared to the CIA group. Furthermore, as depicted in Fig. 8C and D, the body weight of the mice in the SP2509 high-dose group approached that of the control group, and the paw swelling was significantly less pronounced in comparison to the CIA group. ELISA analysis (Fig. 9A) revealed decreased concentrations of IL-1β, TNF-α, and IL-6 in the SP2509 low-dose and high-dose groups compared to the CIA group, thus substantiating the capacity of the drug treatment to attenuate the levels of these inflammatory markers. Western blot assay confirmed the downregulation of LSD1 in mice joints after injection of SP2509 (Fig. 9B). Histopathological examination of the knee joint tissues (Fig. 9C) further confirmed the remarkable reduction in knee joint inflammation in the drug-treated mice as compared to the CIA group. These compelling experimental findings collectively support the premise that SP2509 exerts an inhibitory effect on the progression of rheumatoid arthritis in an in vivo setting.

Discussion

Rheumatoid arthritis (RA) is a widespread systemic autoimmune disorder marked by joint pain, swelling, and stiffness, which often leads to significant physical limitations and a reduced quality of life. The primary pathological feature of RA is synovitis, frequently accompanied by inflammatory cell infiltration, cartilage degradation, and extensive microvascular hyperplasia [30, 31]. Historically, RA treatment relied on synthetic disease-modifying anti-rheumatic drugs (DMARDs) prior to the emergence of targeted therapies [32, 33]. In the past three decades, the introduction of biologic agents has transformed RA treatment [34, 35]. Despite the availability of these new treatments, many patients still do not achieve remission [36, 37], underscoring the need for fresh therapeutic targets.

RA triggers various changes in the synovium, including the infiltration of adaptive immune cells. Nevertheless, the most notable transformations involve the expansion of SFs [38]. In healthy joints, SFs uphold the equilibrium of synovial fluid and extracellular matrix by generating components like lubricin and hyaluronic acid [39]. However, RA alters SFs behavior by prompting them to acquire an aggressive phenotype. These transformed SFs play a

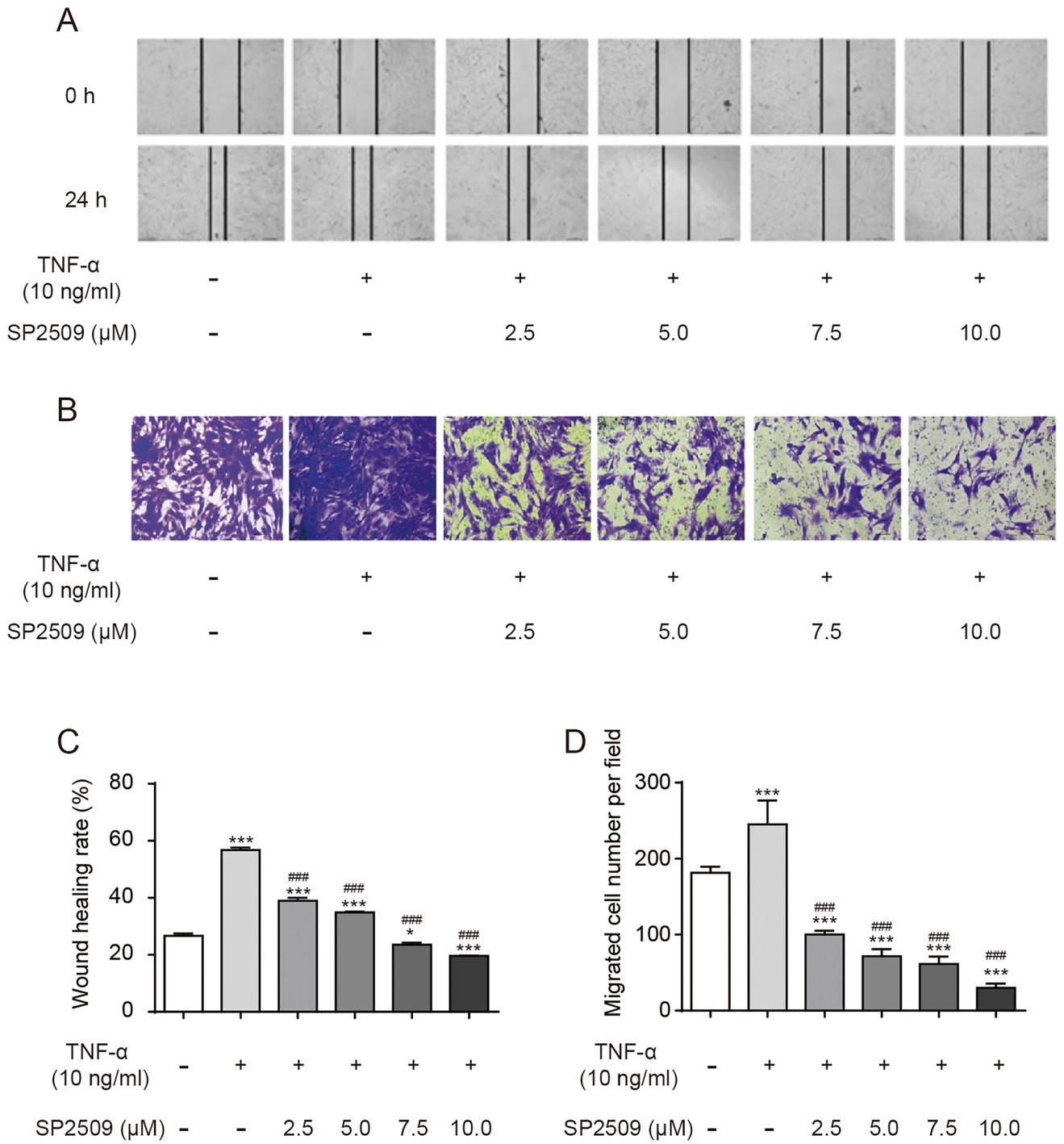

Fig. 7 SP2509 suppressed the migrative capability of MH7A. **A** Wound healing assay is performed, and cells around the scratch are photographed at corresponding time. **B** Transwell assay is performed, and migrated cells are photographed at corresponding time. **C** The histogram shows the alternation of wound healing rate. **D** The histogram shows the alternation of migrated cell numbers. Data is presented as mean ± SD for three independent assays. $*p < 0.05$, $**p < 0.01$, $***p < 0.001$ compared to the Blank group. $\#p < 0.05$, $\#\#p < 0.01$, $\#\#\#p < 0.001$ compared to the TNF-α group

pivotal role in the formation of the RA pannus, an inflammatory, invasive synovial mass responsible for the erosive damage seen in advanced RA [39–41]. Within the pannus, RASFs produce MMPs that degrade various cartilage and support structure proteins, further facilitating pannus growth and invasion [42]. Additionally, RASFs contribute to the inflammatory milieu by generating cytokines like IL-6, granulocyte-macrophage colony-stimulating factor

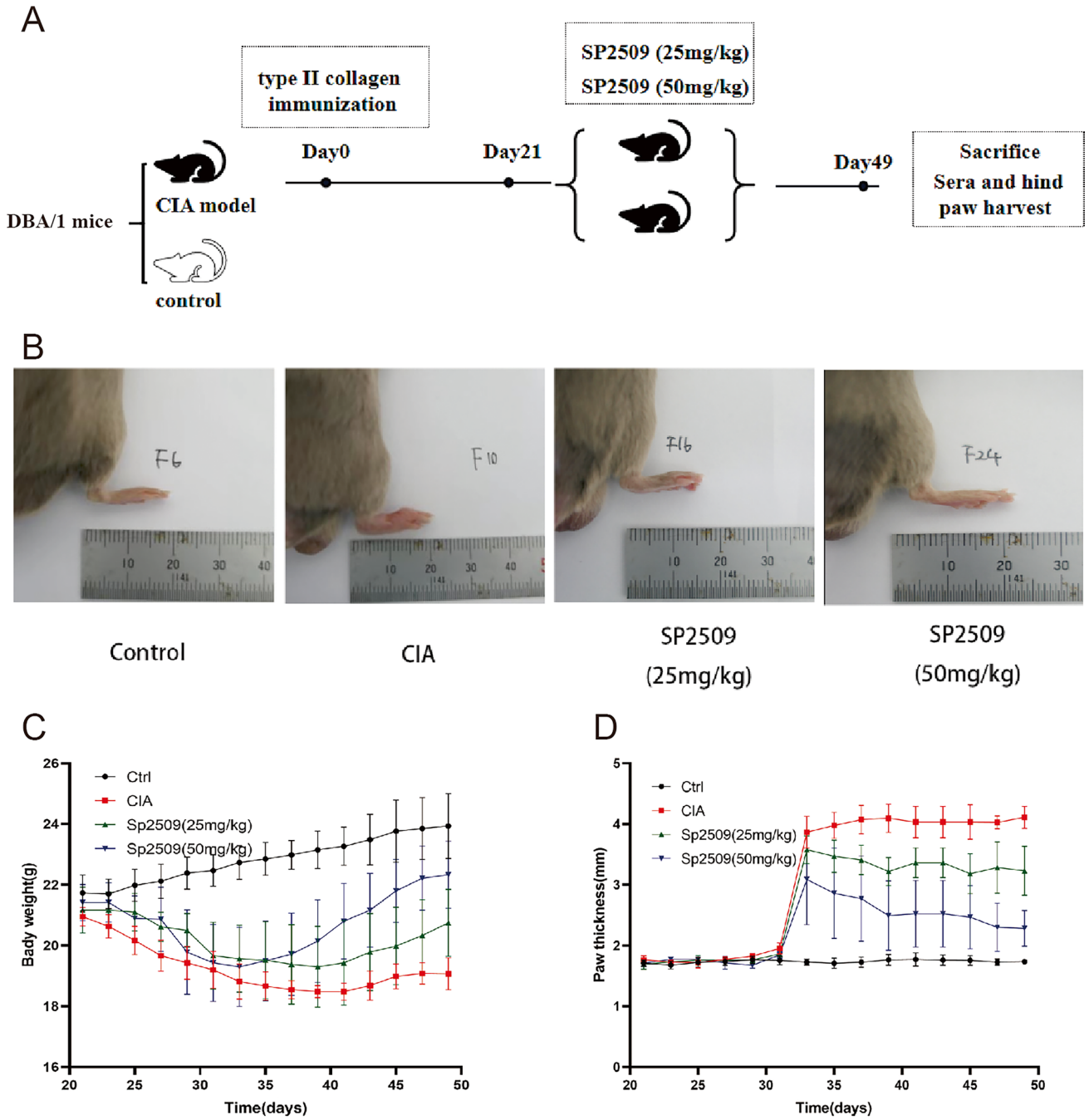

Fig. 8 SP2509 prevented the RA development in the CIA models. **A** Schematic diagram of the experimental schedule for establishing the CIA model and drug treatment (SP2509 high-dose group and SP2509 low-dose group). **B** Photographs of representative paws in each group. **C**, **D** Changes in body weight and paw swelling of mice in each group in animal experiments ($n = 6$)

(GM-CSF), C-C motif chemokine ligand 2 (CCL2), and IL-8 [43]. Moreover, RASFs also release receptor activator of nuclear factor kappa-B ligand (RANKL) to promote osteoclast formation [44, 45]. Therefore, it is crucial to identify effective targets for inhibiting the overactive FLS in the context of RA treatment.

LSD1, a well-established histone demethylase, orchestrates gene transcription and chromatin configuration through epigenetic alterations [46]. Extensive research has unveiled its overexpression in a myriad of tumor types, including gastric cancer, esophageal cancer, breast cancer, and lung cancer [14, 47, 48]. In both hormone-dependent

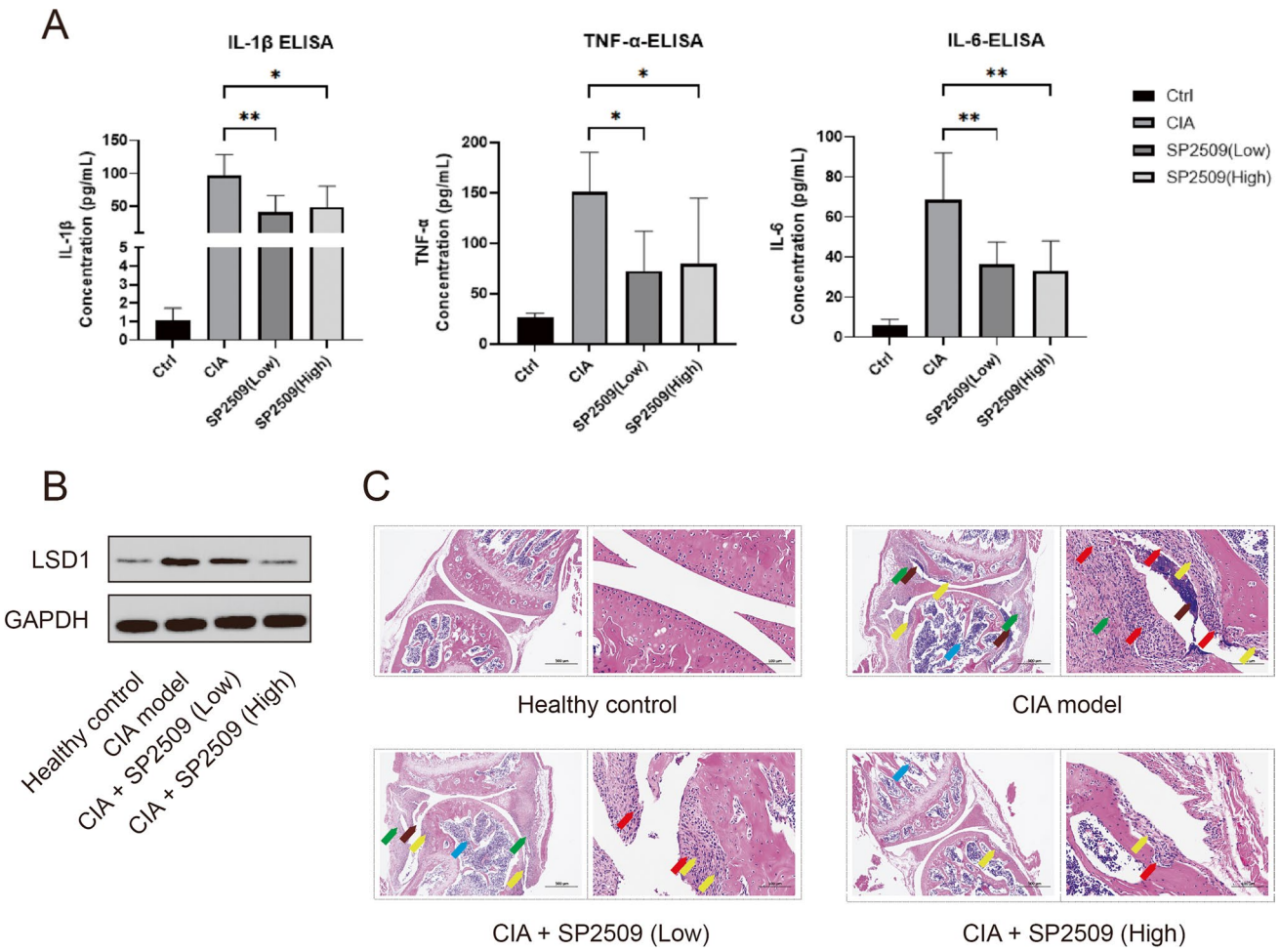

Fig. 9 SP2509 reduces inflammatory cytokine expression and alleviates pathological symptoms in the CIA models. **A** The levels of pro-inflammatory cytokines, including IL-6, TNF-α, and IL-1β, are assessed in the serum of mice from each group using ELISA. **B** Western blot assay shows the expression of LSD1 in RA joint decreases after injection of SP2509. **C** Histopathological examination of knee joint tissues in mice from each group, along with inflammation severity scores. Brown arrows indicate fragmented tissue within the joint cavity, yellow arrows point to blood vessels covered with minimal proliferative connective tissue, green arrows indicate proliferative connective tissue, red arrows represent infiltrating lymphocytes, and blue arrows indicate fragments of trabecular bone. Data is presented as mean ± SD for six samples

and hormone-independent cancers, LSD1 assumes a pivotal role in fostering cell proliferation and development, while concurrently fueling cell migration, invasion, and metastasis through the induction of epithelial-mesenchymal transition (EMT) [49, 50]. RASFs exhibit traits akin to tumor cells, featuring migration and invasion capabilities, which may be regulated by LSD1. Previous research conducted by our team has demonstrated the capacity of microRNA-155 regulation in controlling LSD1 expression, resulting in the inhibition of pro-inflammatory factor release [51]. Subsequently, it was reported that microRNA-137 regulates LSD1 in RASFs, activating RE1 silencing transcription factor (REST) through demethylation, which, in turn, triggers increased levels of pro-inflammatory factors in RASFs [52]. Additionally, the expression of LSD1 in CD4 + T cells has been shown to impact their activation, thereby influencing the progression of RA [18]. These collective findings underscore the significant role of LSD1 in the development of RA.

In our investigation, we initially verified a marked upregulation of LSD1 expression in RA synovial tissues when compared to healthy and OA tissues. To further substantiate these findings, we employed the well-established cell model using TNF-α-treated MH7A cells, which demonstrated a time-dependent increase in LSD1 expression. Considering that silencing LSD1 resulted in the attenuation of INOS expression, we were prompted to explore the potential role of LSD1 antagonists in regulating RASFs. In this context, SP2509, a selective LSD1 inhibitor that has been employed to suppress tumors in various cancer types [53–56], captured our interest. SP2509 exhibited

a concentration-dependent inhibition of TNF-α-induced MH7A cell proliferation while concurrently suppressing LSD1 protein levels. As expected, SP2509 had a significant impact on a range of proteins associated with various cellular processes. Inflammation-related proteins, like INOS and COX-2, proliferation-associated protein PCNA, apoptosis-related proteins such as Bcl-2, Bax, and Caspase3, metalloproteinases like MMP2 and MMP9, and autophagy-related proteins including LC3, Beclin1, ATG5, and ATG7, were all notably modulated by SP2509. These effects were particularly evident in counteracting the adverse changes induced by TNF-α. Furthermore, SP2509 exhibited a concentration-dependent inhibition of the migratory and invasive capabilities of MH7A cells when exposed to inflammatory conditions. In a murine model of CIA, SP2509 treatment substantially improved the progression of RA, leading to a reduction in the expression of pro-inflammatory cytokines and the alleviation of joint pathology. These findings emphasize the crucial role of LSD1 in the context of RA and suggest that SP2509 holds therapeutic promise for this condition.

Conclusions

In conclusion, our investigation involved an evaluation of LSD1 expression in RA tissues relative to normal and OA tissues. It was revealed that SP2509, a selective LSD1 inhibitor, had the capacity to modulate the expression of proteins associated with inflammation, proliferation, apoptosis, and autophagy in an RASF cell model. This inhibition led to reduced cell migration in vitro, as well as the alleviation of pro-inflammatory cytokines and the pathological symptoms in RA mice. These findings underscore the critical role of LSD1 in the context of RA and offer a promising therapeutic avenue in the form of SP2509 for this condition.

Supplementary Information The online version contains supplementary material available at https://doi.org/10.1007/s12026-024-09486-5.

Author contribution Z.Y. and H.Z. conceptualized the study; Z.Y. and P.L. developed the methodology; Y.H. and D.G. performed the software tasks; Z.Y., W.L., and H.Z. validated the findings; F.X. conducted formal analysis; L.L. carried out the investigation; J.L. provided resources; Z.Y. curated the data; Z.Y. wrote the original draft; W.L. and H.Z. reviewed and edited the manuscript; F.X. visualized the data; H.Z. supervised the project; Z.Y. and H.Z. administered the project; Z.Y., W.L., and H.Z. acquired funding. All authors have read and agreed to the published version of the manuscript.

Funding The study was supported by grants from the Nantong First People's Hospital Provincial and Ministerial Level High-level Science and Technology Project Cultivation Fund granted for Ziliang Yu (YPYJJYB23002), the Nantong Youth Medical Expert Project granted for Haiping Zhang, and the Research Project of Nantong Science & Technology Bureau (JC22022029).

Data availability No datasets were generated or analyzed during the current study.

Declarations

Competing interests The authors declare no competing interests.

References

1. Babaahmadi M, et al. Rheumatoid arthritis: the old issue, the new therapeutic approach. Stem Cell Res Ther. 2023;14(1):268.
2. Murayama MA, et al. Chemokines and chemokine receptors as promising targets in rheumatoid arthritis. Front Immunol. 2023;14:1100869.
3. Collaborators GRA. Global, regional, and national burden of rheumatoid arthritis, 1990–2020, and projections to 2050: a systematic analysis of the global burden of Disease Study 2021. Lancet Rheumatol. 2023;5(10):e594–610.
4. Wei M, Chu CQ. Prediction of treatment response: personalized medicine in the management of rheumatoid arthritis. Best Pract Res Clin Rheumatol. 2022;36(1):101741.
5. Tsaltskan V, Firestein GS. Targeting fibroblast-like synoviocytes in rheumatoid arthritis. Curr Opin Pharmacol. 2022;67:102304.
6. Wu Z, et al. Fibroblast-like synoviocytes in rheumatoid arthritis: surface markers and phenotypes. Int Immunopharmacol. 2021;93:107392.
7. Jang S, Kwon EJ, Lee JJ. Rheumatoid Arthritis: pathogenic roles of diverse immune cells. Int J Mol Sci. 2022;23(2):905.
8. Cheng X, et al. Components of the sympathetic nervous system as targets to modulate inflammation - rheumatoid arthritis synovial fibroblasts as neuron-like cells? J Inflamm (Lond). 2023;20(1):9.
9. Wang J, et al. Single-cell communication patterns and their intracellular information flow in synovial fibroblastic osteoarthritis and rheumatoid arthritis. Immunol Lett. 2023;263:1–13.
10. Wang Z, et al. Tyro3 receptor tyrosine kinase contributes to pathogenic phenotypes of fibroblast-like synoviocytes in rheumatoid arthritis and disturbs immune cell balance in experimental arthritis. Clin Immunol. 2023;255:109753.
11. Makuch S, Więcek K, Woźniak M. The immunomodulatory and anti-inflammatory effect of curcumin on immune cell populations, cytokines, and in vivo models of rheumatoid arthritis. Pharmaceuticals (Basel). 2021;14(4):309.
12. Forneris F, et al. LSD1: oxidative chemistry for multifaceted functions in chromatin regulation. Trends Biochem Sci. 2008;33(4):181–9.
13. Wang Y, et al. LSD1 is required for euchromatic origin firing and replication timing. Signal Transduct Target Ther. 2022;7(1):102.
14. Dong J, et al. A comprehensive comparative study on LSD1 in different cancers and tumor specific LSD1 inhibitors. Eur J Med Chem. 2022;240:114564.
15. Ma T, et al. KDM1A/LSD1 as a promising target in various diseases treatment by regulating autophagy network. Biomed Pharmacother. 2022;148:112762.
16. Gu F, et al. Biological roles of LSD1 beyond its demethylase activity. Cell Mol Life Sci. 2020;77(17):3341–50.
17. Kim D, et al. PKCα-LSD1-NF-κB-Signaling Cascade is crucial for Epigenetic Control of the inflammatory response. Mol Cell. 2018;69(3):398–e4116.
18. Liu W, et al. Knockdown of LSD1 ameliorates the severity of rheumatoid arthritis and decreases the function of CD4 T cells in mouse models. Int J Clin Exp Pathol. 2018;11(1):333–41.

19. Guo Y, et al. CD40L-Dependent pathway is active at various stages of Rheumatoid Arthritis Disease Progression. J Immunol. 2017;198(11):4490–501.
20. Walsh AM, et al. Triple DMARD treatment in early rheumatoid arthritis modulates synovial T cell activation and plasmablast/plasma cell differentiation pathways. PLoS One. 2017;12(9):e0183928.
21. Brand DD, Latham KA, Rosloniec EF. Collagen-induced arthritis. Nat Protoc. 2007;2(5):1269–75.
22. Kondo N, Kuroda T, Kobayashi D. Cytokine networks in the pathogenesis of rheumatoid arthritis. Int J Mol Sci, 2021. 22(20).
23. McConkey B, et al. Effects of gold, dapsone, and prednisone on serum C-reactive protein and haptoglobin and the erythrocyte sedimentation rate in rheumatoid arthritis. Ann Rheum Dis. 1979;38(2):141–4.
24. Blaschke S, et al. Haptoglobin-α1, -α2, vitamin D-binding protein and apolipoprotein C-III as predictors of etanercept drug response in rheumatoid arthritis. Arthritis Res Ther. 2015;17(1):45.
25. Osborn TM, et al. Decreased levels of the gelsolin plasma isoform in patients with rheumatoid arthritis. Arthritis Res Ther. 2008;10(5):R117.
26. Nandi A, et al. The abundant phytocannabinoids in rheumatoid arthritis: therapeutic targets and molecular processes identified using Integrated Bioinformatics and Network Pharmacology. Life (Basel). 2023;13(3):700.
27. Hemmatzadeh M, et al. The role of immune regulatory molecules in rheumatoid arthritis: implication for etiopathogenesis and prospective for treatment. J Cell Physiol. 2022;237(9):3541–53.
28. Irwin MR, Straub RH, Smith MT. Heat of the night: sleep disturbance activates inflammatory mechanisms and induces pain in rheumatoid arthritis. Nat Rev Rheumatol. 2023;19(9):545–59.
29. Edilova MI, Akram A, Abdul-Sater AA. Innate immunity drives pathogenesis of rheumatoid arthritis. Biomed J. 2021;44(2):172–82.
30. Guo Q, et al. Rheumatoid arthritis: pathological mechanisms and modern pharmacologic therapies. Bone Res. 2018;6:15.
31. Alivernini S, Firestein GS, McInnes IB. The pathogenesis of rheumatoid arthritis. Immunity. 2022;55(12):2255–70.
32. Sepriano A, et al. Safety of synthetic and biological DMARDs: a systematic literature review informing the 2022 update of the EULAR recommendations for the management of rheumatoid arthritis. Ann Rheum Dis. 2023;82(1):107–18.
33. Aletaha D, Smolen JS. Diagnosis and management of rheumatoid arthritis: a review. JAMA. 2018;320(13):1360–72.
34. Ding Q, et al. Signaling pathways in rheumatoid arthritis: implications for targeted therapy. Signal Transduct Target Ther. 2023;8(1):68.
35. Bergstra SA, et al. Efficacy, duration of use and safety of glucocorticoids: a systematic literature review informing the 2022 update of the EULAR recommendations for the management of rheumatoid arthritis. Ann Rheum Dis. 2023;82(1):81–94.
36. Lortholary O, et al. Infectious complications of rheumatoid arthritis and psoriatic arthritis during targeted and biological therapies: a viewpoint in 2020. Ann Rheum Dis. 2020;79(12):1532–43.
37. Sparks JA, et al. Comparative effectiveness of treatments for rheumatoid arthritis in clinical practice: a systematic review. Semin Arthritis Rheum. 2023;62:152249.
38. Nygaard G, Firestein GS. Restoring synovial homeostasis in rheumatoid arthritis by targeting fibroblast-like synoviocytes. Nat Rev Rheumatol. 2020;16(6):316–33.
39. Neumann E, et al. Rheumatoid arthritis progression mediated by activated synovial fibroblasts. Trends Mol Med. 2010;16(10):458–68.
40. Dimitroulas T, et al. Biologic therapies and systemic bone loss in rheumatoid arthritis. Autoimmun Rev. 2013;12(10):958–66.
41. Tsuchiya H, Ota M, Fujio K. Multiomics landscape of synovial fibroblasts in rheumatoid arthritis. Inflamm Regen. 2021;41(1):7.
42. Senolt L, et al. S100A4 is expressed at site of invasion in rheumatoid arthritis synovium and modulates production of matrix metalloproteinases. Ann Rheum Dis. 2006;65(12):1645–8.
43. Komatsu N, Takayanagi H. Mechanisms of joint destruction in rheumatoid arthritis - immune cell-fibroblast-bone interactions. Nat Rev Rheumatol. 2022;18(7):415–29.
44. Kim HR, et al. Reciprocal activation of CD4 + T cells and synovial fibroblasts by stromal cell-derived factor 1 promotes RANKL expression and osteoclastogenesis in rheumatoid arthritis. Arthritis Rheumatol. 2014;66(3):538–48.
45. Kikyo N. Circadian regulation of macrophages and osteoclasts in rheumatoid arthritis. Int J Mol Sci, 2023. 24(15).
46. Shi YJ, et al. Regulation of LSD1 histone demethylase activity by its associated factors. Mol Cell. 2005;19(6):857–64.
47. Venkata PP, et al. Pharmacological inhibition of KDM1A/LSD1 enhances estrogen receptor beta-mediated tumor suppression in ovarian cancer. Cancer Lett. 2023;575:216383.
48. Shao TL, Ting RT, Lee MC. Identification of Lsd1-interacting non-coding RNAs as regulators of fly oogenesis. Cell Rep. 2022;40(9):111294.
49. Ferrari-Amorotti G, et al. Inhibiting interactions of lysine demethylase LSD1 with snail/slug blocks cancer cell invasion. Cancer Res. 2013;73(1):235–45.
50. Carmichael CL, et al. The EMT modulator SNAI1 contributes to AML pathogenesis via its interaction with LSD1. Blood. 2020;136(8):957–73.
51. Yu Z, et al. MicroRNA-155 participates in the expression of LSD1 and proinflammatory cytokines in rheumatoid synovial cells. Mediators Inflamm. 2020;2020:4092762.
52. Sun W, Zhang Y, Wang G. MicroRNA-137-mediated inhibition of lysine-specific demethylase-1 prevents against rheumatoid arthritis in an association with the REST/mTOR axis. Mol Pain. 2021;17:17448069211041847.
53. Tokarsky EJ, et al. Mitochondrial dysfunction is a driver of SP-2509 Drug Resistance in Ewing Sarcoma. Mol Cancer Res. 2022;20(7):1035–46.
54. Jiang A, et al. SP2509, a selective inhibitor of LSD1, suppresses Retinoblastoma Growth by Downregulating β-catenin signaling. Invest Ophthalmol Vis Sci. 2022;63(3):20.
55. Wu K, Woo SM, Kwon TK. The histone lysine-specific demethylase 1 inhibitor, SP2509 exerts cytotoxic effects against Renal Cancer cells through downregulation of Bcl-2 and Mcl-1. J Cancer Prev. 2020;25(2):79–86.
56. Pishas KI, et al. Therapeutic targeting of KDM1A/LSD1 in Ewing Sarcoma with SP-2509 engages the endoplasmic reticulum stress response. Mol Cancer Ther. 2018;17(9):1902–16.